Supplementary Information for

Bioinspired iron-loaded polydopamine nanospheres as green flame retardant for epoxy resin via free radical scavenging and catalytic charring

Lu Zhang,[a,b] Qi Wang,[a,b] Rong-Kun Jian,[a,c] and De-Yi Wang[a,*]

[a] *IMDEA Materials Institute, Calle Eric Kandel, 2, 28906 Getafe, Madrid, Spain*

[b] *E.T.S. de Ingenieros de Caminos, Universidad Politécnica de Madrid, Calle Profesor Aranguren 3, 28040 Madrid, Spain*

[c] *College of Chemistry and Materials Science, Fujian Normal University, Shangsan Road 8, 350007 Fuzhou, Fujian, China*

**Corresponding author: De-Yi Wang, Tel.: 0034-917871888, E-mail: deyi.wang@imdea.org*

TGA curve of Fe-PDA under air atmosphere (**Figure S1**) clearly shows that the decomposition of Fe-PDA mainly happens above 150 °C (which is the second stage curing temperature for EP composites) in air.

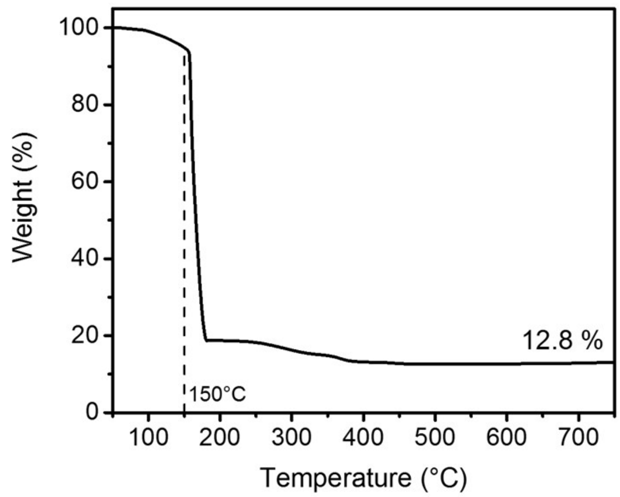

Figure S1. TGA curve of Fe-PDA under air atmosphere.

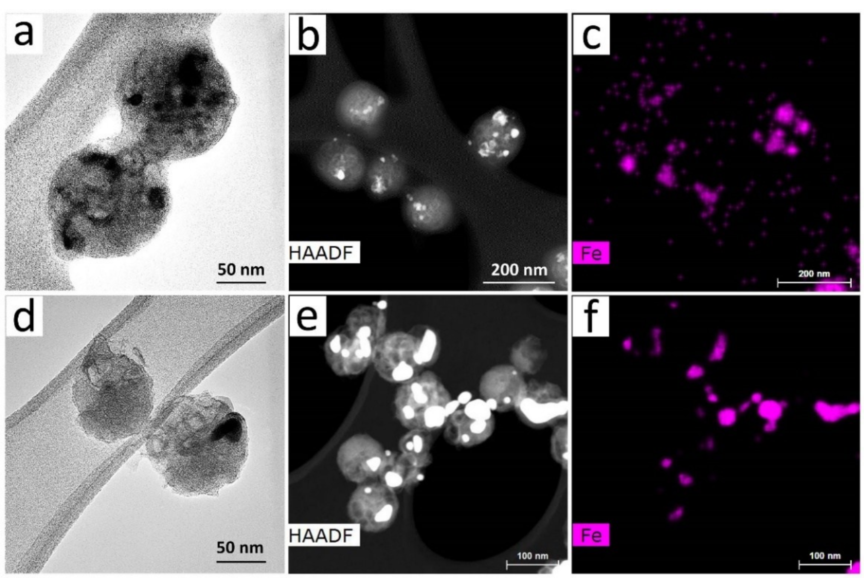

Figure S2. TEM, HAADF image and Fe element mapping of (a-c) Fe/C-PDA-5, (d-f) Fe/C-PDA-10.

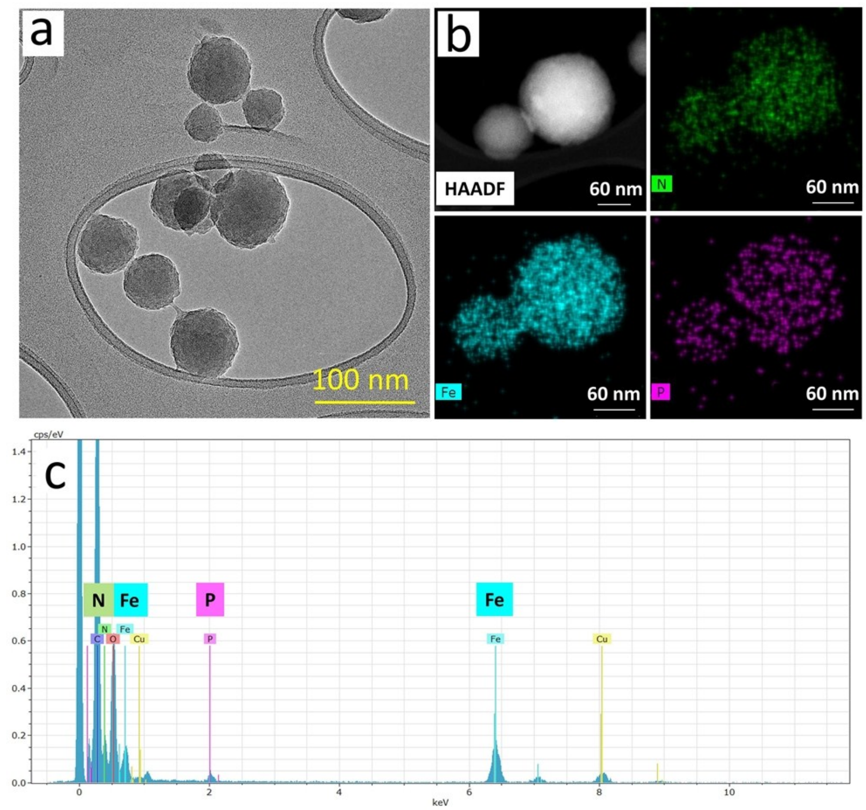

Figure S3. (a) TEM image, (b) HAADF image, element mappings and (c) EDS spectra of DOPO@Fe-PDA.

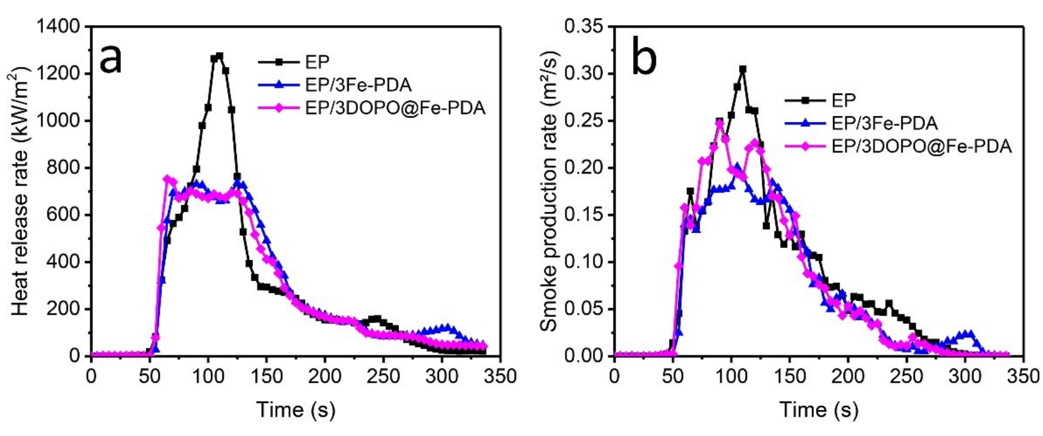

Figure S4. (a) HRR, (b) SPR curves of EP, EP/3Fe-PDA and EP/3DOPO@Fe-PDA.

As seen from TGA results in **Figure S5,** Fe-PDA and DOPO@Fe-PDA showed similar carbonization effect in epoxy.

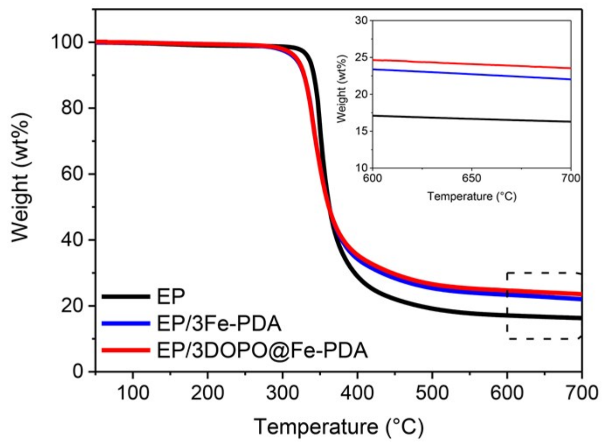

Figure S5. TGA results of EP, EP/3Fe-PDA and EP/3DOPO@Fe-PDA in N_2 atmosphere.

Digital photos of the char residues show an apparent difference between neat EP and the flame retardant composites. The compact and multiple layered char acts as an effective physical barrier to protect the underlying polymeric substrate. The red color of the surface layer is attributed to the formation of iron oxides when exposed directly to air under a high temperature.

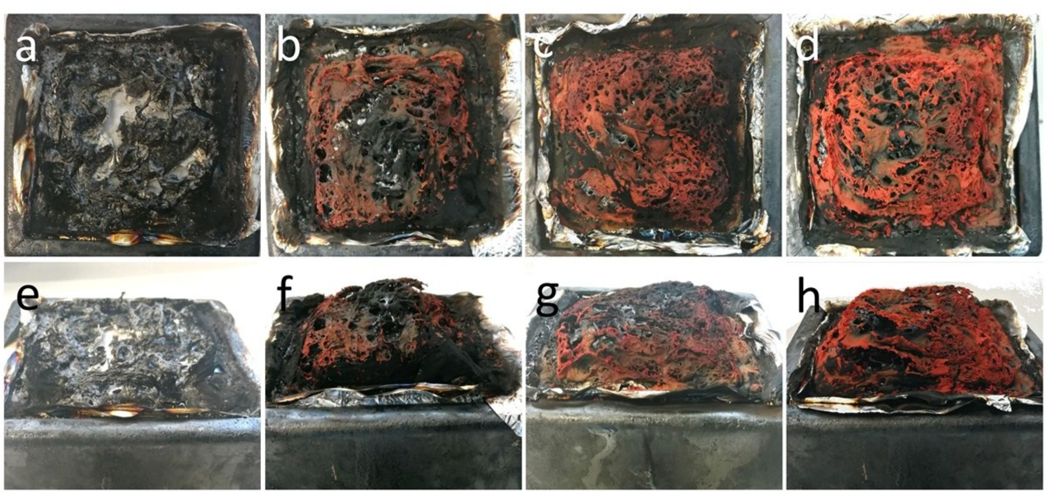

Figure S6. Digital photos of residues after cone calorimeter test from top and side views for (a,e) EP, (b,f) EP/1Fe-PDA, (c,g) EP/3Fe-PDA and (d,h) EP/5Fe-PDA.

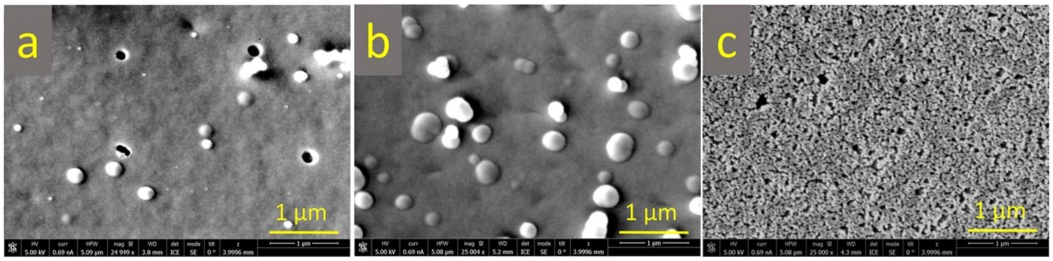

Figure S7. High-magnification SEM images of residues for (a) EP/1Fe-PDA, (b) EP/3Fe-PDA and (c) EP/5Fe-PDA.

The char residue of EP/3DOPO@Fe-PDA showed a compact and dense morphology in digital photos (**Figure S8a and b**) and SEM images (**Figure S8d-f**), which was responsible for the reduced heat release rate in cone calorimeter test. Raman curve (**Figure S8c**) of residue from EP/3DOPO@Fe-PDA exhibited a low I_D/I_G value of 2.0. The differences in line shapes of Raman spectra and SEM morphologies between residue from EP/Fe-PDA and EP/DOPO@Fe-PDA indicated the different char formation processes during combustion. In EP/3DOPO@Fe-PDA, the phosphorus remaining in the condensed phase helped reduce the heat release rate by enhancing the charring of polymer and formation of stable polyphosphate structures, which is well understood in other researches related to phosphorus based polymer flame retardancy.[S1]

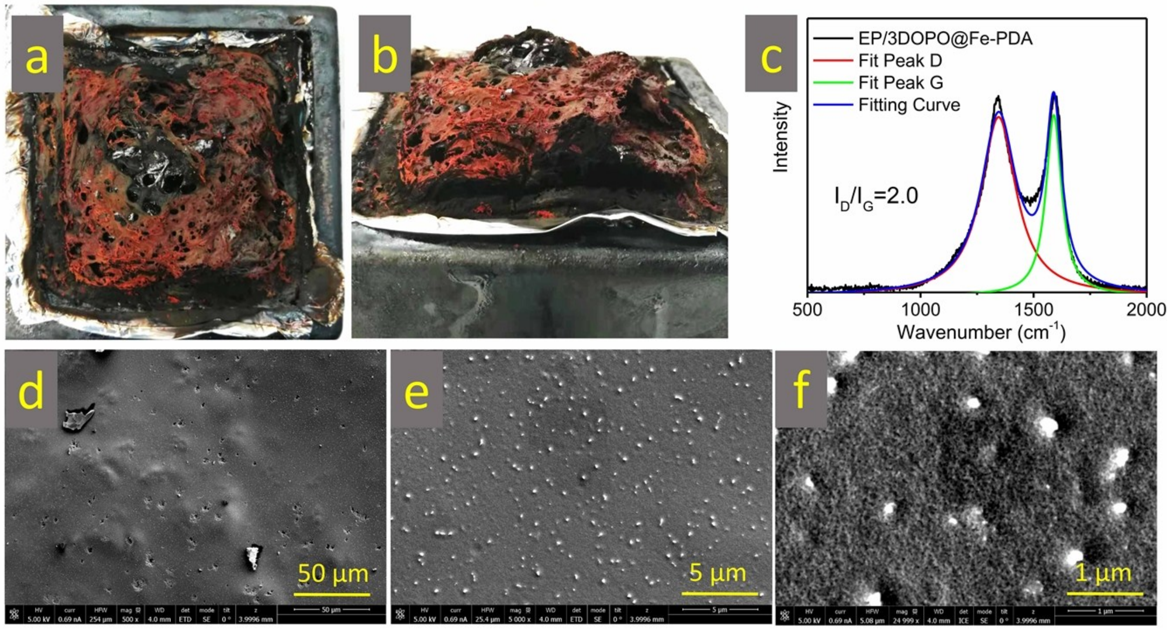

Figure S8. (a,b) Digital photos, (c) Raman curve and (d-f) SEM images of char residue from EP/3DOPO@Fe-PDA.

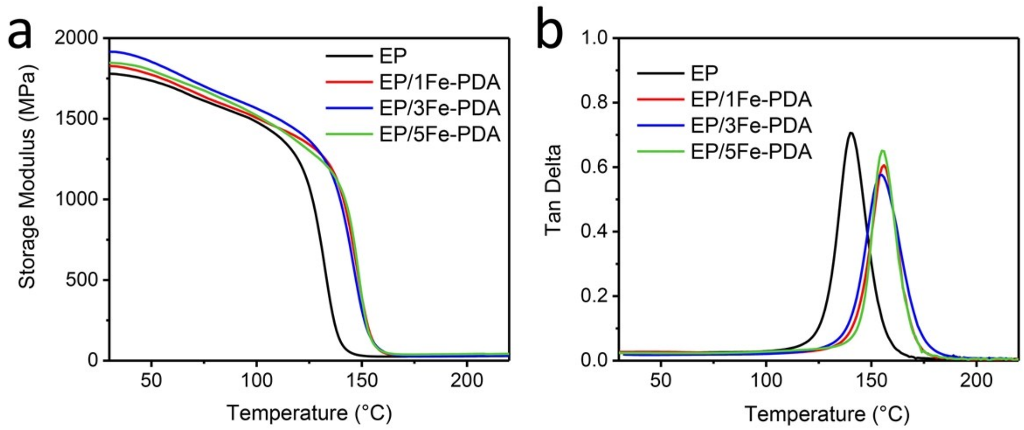

Figure S9. (a) Storage modulus and (b) Tan Delta curves of EP and its nanocomposites.

The influence of Fe-PDA on the curing of EP was investigated by DSC testing. From the dynamic DSC curves **(Figure S11)** of EP and its nanocomposites, it can be seen that the exothermic peak corresponding to curing reaction appears at 165.1 °C for neat EP. The exothermic peak decreases and shifts to a lower temperature for EP/Fe-PDA nanocomposites, indicating the addition of Fe-PDA promotes the curing reaction of EP.[S2,S3]

It is worth noting that abundant catechol moieties and amino groups exist in polydopamine materials,[S4,S5] which can act as catalyst for the curing reaction of EP.[S6,S7]

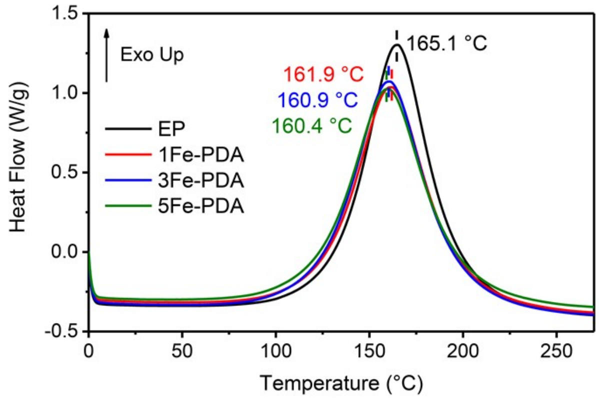

Figure S10. Non-isothermal DSC curves of the curing reaction of EP and its nanocomposites.

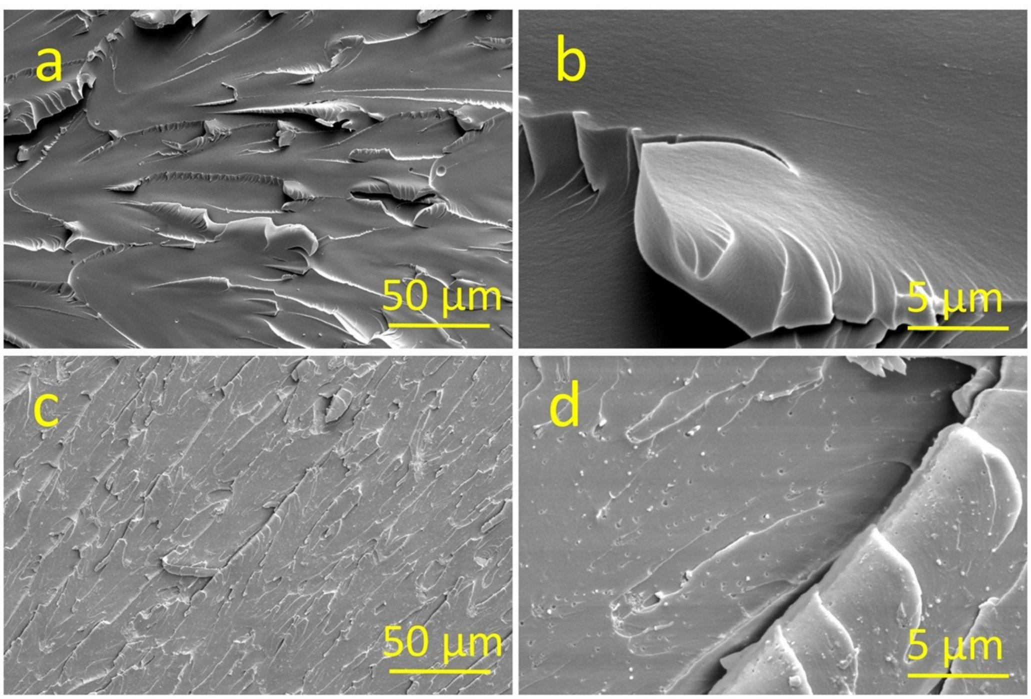

Figure S11. SEM images of freeze-fractured surfaces for (a,b) EP and (c,d) EP/3Fe-PDA.

Reference

S1. B. Schartel, *Materials*, 2010, **3**, 4710-4745. https://doi.org/10.3390/ma3104710.

S2. M. Spontón, L. A. Mercado, J. C. Ronda, M. Galià and V. Cádiz, *Polym. Degrad. Stab.*, 2008, **93**, 2025-2031. https://doi.org/10.1016/j.polymdegradstab.2008.02.014.

S3. X. Qian, L. Song, B. Yu, B. Wang, B. Yuan, Y. Shi, Y. Hu and R. K. K. Yuen, *J. Mater. Chem. A*, 2013, **1**, 6822-6830. https://doi.org/10.1039/C3TA10416H.

S4. J. Liebscher, *Eur. J. Org. Chem.*, 2019, **31-32**, 4976-4994. https://doi.org/10.1002/ejoc.201900445.

S5. J. Liebscher, R. Mrówczyński, H. A. Scheidt, C. Filip, N. D. Haìdade, R. Turcu, A. Bende and S. Beck, *Langmuir*, 2013, **29**, 10539-10548. https://doi.org/10.1021/la4020288.

S6. Y. Tanaka and H. Kakiuchi, *J. Appl. Polym.*, 1963, **7**, 1063-1081. https://doi.org/10.1002/app.1963.070070322.

S7. F. X. Perrin, T. M. H. Nguyen and J. L.Vernet, *Eur. Polym. J.*, 2007, **43**, 5107-5120. https://doi.org/10.1016/j.eurpolymj.2007.09.020.